Confluent hepatic fibrosis in liver cirrhosis: Possible relation with middle hepatic venous drainage

doi: 10.1007/s11604-013-0222-8

Confluent hepatic fibrosis in liver cirrhosis: possible relation with middle hepatic venous drainage

Abstract

Purpose: To retrospectively analyze the location of confluent hepatic fibrosis in relation to the portal and hepatic venous anatomy using multidetector computed tomography (CT) and to clarify the influence of the hepatic venous drainage on confluent fibrosis.

Materials and Methods: The study population consisted of 879 patients diagnosed with cirrhosis: 539 men and 340 women (65.9 ± 10.6 years), 633 patients with Child-Pugh class A, 161 with class B, and 85 with class C. The cause of cirrhosis was hepatitis C (n= 528) and hepatitis B (n= 122) virus infection, alcoholism (n= 114), and others (n= 115). The confluent fibrosis was diagnosed using CT images according to previous reports, and statistically analyzed ($p<.05$).

Results: Thirty-five confluent fibrosis lesions in 30 patients (3.4%) were

identified. The predictive factors were alcoholic cirrhosis (odds ratio, 7.25; p<.0001), Child-Pugh class C (odds ratio, 6.95; p<.0001), and Child-Pugh class B (odds ratio, 2.91; p<.0023). The confluent fibrosis was most frequently seen in the middle hepatic venous drainage area (n= 21), or at the boundary between the medial and anterior segments (n= 17), and each distribution of the location of confluent fibrosis was significantly unequal (p<.0001).

Conclusion: Confluent fibrosis was most commonly located in the middle hepatic venous drainage area.

Keywords: confluent hepatic fibrosis; liver cirrhosis; hepatic venous drainage; alcoholism; Child-Pugh classification

Introduction

Liver fibrosis, a common feature of almost all causes of chronic liver disease, refers to the excess deposition of collagen, proteoglycans, and other macromolecules in the extracellular matrix in response to repetitive liver injury from various causes [1]. Liver fibrosis is considered to be irreversible, but is regarded as a dynamic process with potential for regression [2]. During the progression of fibrosis, the accumulation of proteins in the extracellular matrix promotes the formation of scars that bridge together across adjacent portal triads and central veins, and ultimately, hepatic fibrosis can be demonstrated on computed tomography (CT) or magnetic resonance (MR) imaging as fibrotic septa and bridges in patients with end-stage liver disease [2, 3].

Confluent hepatic fibrosis is considered to be the most extreme stage of fibrosis and is occasionally encountered in patients with end-stage cirrhosis. It is demonstrated as broad fibrotic scars, and the imaging findings have been summarized as a focal, often wedge-shaped mass, with either overlying

capsule retraction or focal flattening of the capsule, most often involving the anterior and medial segment, and less frequently the posterior segment [4, 5]. Ohtomo et al [4] speculated that the mechanism of this change might be related to impaired portal microcirculation, although the intrahepatic portal venous system was grossly patent. After the original reports, several cases showing similar locations of confluent fibrosis were described [6-10]. However, it has not been clarified why the fibrosis of diffuse liver disease, a basically diffuse process, appears preferentially in these particular segments as confluent fibrosis.

It is widely recognized that a decreased or reversed flow of the portal blood supply can be seen when the hepatic venous flow is obstructed [11, 12]. As a result, parenchymal changes similar to those evoked by portal venous flow blockage can be expected, resulting in marked fibrosis in the area with hepatic venous flow disturbance. Furthermore, in cirrhosis, hepatic venous flow disturbance due to the compression and deformity caused by regenerative nodules and fibrosis is one of the most important causes of

portal hypertension [13]. In addition, Ozaki et al [14] previously reported that selective atrophy of middle hepatic venous (MHV) drainage area commonly occurs in hepatitis C-related liver cirrhosis (mostly macronodular cirrhosis). Based on these facts and observations, we speculated that disturbed hepatic venous drainage might be related to the development of confluent fibrosis.

In this study, we retrospectively analyzed the location of confluent fibrosis in relation to the portal venous supply and hepatic venous drainage using multidetector CT so as to clarify the influence of the hepatic venous drainage on confluent fibrosis.

Materials and Methods

Institutional approval was obtained for this retrospective study, and informed consent to use the medical records and materials for this study was obtained from all patients.

Patients

Between October 2002 and August 2009, 1327 consecutive patients with cirrhosis at our institution who underwent upper abdominal dynamic CT to evaluate the stage of their chronic liver injury and to detect any associated hepatocellular carcinoma were investigated. There were 854 men and 473 women with a mean age of 66.2 ± 10.7 years (range, 7-90 years). Four hundred and forty-eight patients were excluded because of difficulty in accurately evaluating the morphology of the liver or the locations based on the portal or hepatic vein due to a history of transcatheter arterial chemoembolization and/or radiofrequency ablation (n= 230), severe deformation or hepatomegaly due to advanced tumor (n= 113), history of hepatectomy (n= 69), an interruption of the scan because of the development of a contrast material-related allergy (n= 20), history of living donor liver transplantation (n= 9), or history of transjugular intrahepatic portosystemic shunt (n= 7). The final study population consisted of 879 patients; 539 men and 340 women with a mean age of 65.9 ± 10.6 years (range, 7-89 years), 633

patients with Child-Pugh class A cirrhosis, 161 patients with Child-Pugh class B cirrhosis and 85 patients with Child-Pugh class C cirrhosis. The cause of cirrhosis was hepatitis C virus infection (n= 528), hepatitis B virus infection (n= 122), alcoholism (n= 114), unknown etiology (n= 36), primary biliary cirrhosis (PBC) (n= 31), non-alcoholic steatohepatitis (NASH) (n= 24), autoimmune hepatitis (AIH) (n= 15), hepatitis C and B virus infection (n= 3), Budd-Chiari syndrome (n= 3), hepatitis C virus infection and alcoholism (n= 2), or Wilson's disease (n= 1). More details are noted in Table 1. Diagnosis of cirrhosis was based on histology in 626 patients: percutaneous liver biopsy (n= 591), hepatectomy for hepatocellular carcinoma (n= 32), and liver transplantation (n= 3). The histological data were adjunctively referred to in the patients who underwent hepatectomy or liver transplantation if confluent fibrosis was detected. In the remaining 253 patients [hepatitis C virus infection (n= 187), hepatitis B virus infection (n= 51), alcoholism (n= 12), and Budd-Chiari syndrome (n= 3)], a clinical diagnosis of cirrhosis was based on a combination of imaging findings (ultrasound, CT, and/or MR

imaging) [15-17], upper gastrointestinal endoscopic findings (esophageal and/or gastric varices), abnormal laboratory data (prolonged prothrombin time, decreased platelet count, abnormal serum albumin and cholesterol levels, increased total bilirubin and γ-globulin levels, specific antinuclear antibody, and so on), and clinical presentation (cutaneous spider angiomas, abdominal subcutaneous portosystemic shunts, ascites, and hepatic encephalopathy, and so on) or clinical history (drinking history, other disease). Most of these patients were not candidates for liver biopsy because of advanced end-stage cirrhosis or refusal of biopsy.

Imaging Techniques

Abdominal dynamic CT images were obtained with a LightSpeed Ultra 16 (GE Medical Systems, USA) (n= 723) or with a LightSpeed VCT 64 (GE Medical Systems, USA) (n= 156), which was introduced in March 2008. Images obtained with the LightSpeed Ultra 16 were acquired through the liver in a craniocaudal direction with a 1.5×16 beam collimation. Other CT

parameters were as follows: 300-350 mAs; 120 kVp; detector collimation, 2.5 mm; table speed, 14 mm per rotation; gantry rotation time, 0.5 s; reconstruction section thickness of 2.5 mm and a reconstruction interval of 2.5 mm. Before each scan, patients were instructed to breathe in and hold during the scanning. Following precontrast CT, a dynamic contrast study was performed 30s (arterial phase), 60s (portal phase), and 120s (equilibrium-phase) after the completion of an intravenous injection of 600 mgI/kg of nonionic contrast material (Iomeron 350 [Eisai, Tokyo, Japan]) at a rate of 3-4 mL/s. Using these acquisition parameters, the approximate mean volume CT dose index was 18.2 mGy and the dose length product was 550.1 mGy-cm per scan.

Images obtained with a LightSpeed VCT 64 were acquired through the liver in a craniocaudal direction with a 0.625 × 64 beam collimation. Other CT parameters were as follows: Auto mA (GE Healthcare; 10–700 mA, Noise Index of 8.0); the remainder was the same as noted above. Following precontrast CT, a dynamic contrast study was performed using the Smart

Prep option (automated software with scan triggering; GE Medical Systems) and 600 mgI/kg of nonionic contrast material (Iomeron 350) was administered for thirty seconds. The arterial phase scanning was initiated just after a 200 Hounsfield unit enhancement threshold was achieved in the aorta at the level of the celiac artery. The portal and equilibrium-phase scanning was performed at 35-second and 115-second delays, respectively, from the time of initiation of the arterial phase scanning. Using these acquisition parameters, the approximate mean volume CT dose index was 18.7 mGy and the dose length product was 570.3 mGy-cm per scan.

Definition of confluent hepatic fibrosis

The presence of confluent fibrosis was evaluated based on the original report of Ohtomo et al [4]. The imaging findings are as follows: the shape is wedge-shaped, peripheral and band-shaped lesions remote from the central portion of the liver, or segmental involvement. On precontrast CT, it usually shows hypoattenuation relative to the surrounding liver parenchyma. The

lesion might be isoattenuating when the density of surrounding liver parenchyma is lower than usual. On the arterial phase, it may show a variety of enhancement patterns on CT and MR imaging [6, 17]. A variable degree of delayed enhancement is commonly seen on the equilibrium-phase [6, 18]. The lesions show varying degrees of parenchymal shrinkage of the involved area and capsule retraction. No calcification or dilatation of the intrahepatic biliary ducts is seen. The portal trunk and major hepatic vein including its major branches were confirmed to be patent to exclude morphological changes due to thrombus or tumor invasion. CT images in all 879 patients were interpreted and the presence of confluent fibrosis was identified retrospectively by 3 experienced abdominal radiologists (two with more than 10 and the other with more than 30 years of experience each in liver imaging). All images were analyzed subjectively and independently by these 3 radiologists.

Definition of hepatic segments

In cases with confluent fibrosis, its location was categorized according to the hepatic segmentation defined by the Couinaud system [19]; lateral, medial, anterior, and posterior segments, and caudate lobe. The portal vein was traced from the main portal trunk to peripheral branch using a viewer (EV Insite Version 2.10.7.91, PSP Corporation, Tokyo, Japan) during the portal phase of axial CT, and the location was categorized based on the branches supplying the lesion.

The location of confluent fibrosis was also categorized according to the hepatic venous branches. They were classified as left, middle, and right hepatic venous (LHV, MHV, and RHV) drainage areas [20, 21]. The hepatic veins were traced from the point of convergence with the inferior vena cava, or the point of convergence of the MHV and LHV up to the hepatic surface during the portal phase or the equilibrium-phase of axial CT using the viewer, and the drainage branches to the lesion were identified. The reached branch of the major hepatic vein was defined as each hepatic venous drainage area. The vessels and their location were identified by the same

three radiologists in consensus. Representative cases of confluent fibrosis are shown in Figures 1 and 2.

Statistical analysis

To assess interobserver variability, k statistics were applied. A k value of up to 0.20 was considered to indicate slight agreement; a k value of 0.21–0.40, fair agreement; a k value of 0.41–0.60, moderate agreement; a k value of 0.61–0.80, substantial agreement; and a k value of 0.81 or greater, almost perfect agreement. The Mann-Whitney U test was used to compare the distribution of age. Chi-square test or Fisher's exact test (if the observed frequency of cases was less than five) was used for categorical variables (sex, Child-Pugh classification, and cause of cirrhosis). The cause was categorized as alcoholism or others for analysis using Fisher's exact test, because the numbers of cases with confluent fibrosis due to each cause of cirrhosis were too few to obtain reliable statistical results. Stepwise multiple logistic regression analysis by means of forward selection was used to identify

significant factors of confluent hepatic fibrosis. The significant variables in the univariable analyses were included. The cause was categorized as alcoholism or others for the same reason mentioned above. The chi-square test for goodness-of-fit with Yates' continuity correction was used to access the distribution of the location of the confluent fibrosis based on the portal blood supply or hepatic venous drainage. Cases with the lesions infrequently observed were categorized as others if needed. All analyses were performed with statistical software (Dr. SPSS II for Windows, version 11.0.1 J; SPSS, Chicago, Ill), and $p < .05$ was considered statistically significant.

Thirty-five focal confluent fibrosis lesions in 30 patients (3.4%) were identified. Twenty-five patients (83.3%) had a single lesion, 5 (16.7%) had two lesions, and no patient had three or more lesions. In three patients, it was confirmed histologically by liver transplantation and in one by partial hepatectomy for hepatocellular carcinoma at a different location. They were 24 men and 6 women (Fisher's exact test, p=0.036) with a mean age of 62.6 ± 10.3 years (range, 44-84 years) (Mann-Whitney U test, p=0.039). The cause

of the confluent fibrosis was alcoholism (n= 17/114) (14.9%), AIH (n= 1/15) (6.7%), PBC (n=1/31) (3.2%), unknown etiology (n=1/36) (2.8%), or hepatitis C virus infection (n= 10/528) (1.9%). They were classified as Child-Pugh class A cirrhosis (n=11/633) (1.7%), Child-Pugh class B cirrhosis (n=9/161) (5.6%), and Child-Pugh class C cirrhosis (n=10/85) (11.8%). Stepwise multivariate logistic regression analysis included the variables for all clinical data. The results showed that the significant predictive factors of confluent fibrosis were alcoholic cirrhosis (odds ratio, 7.251; $p < 0.001$; 95% confidence interval (CI), 3.366-15.619), Child-Pugh class C (odds ratio, 6.946; $p < 0.001$; 95% CI, 2.765-17.446), and Child-Pugh class B (odds ratio, 2.914; $p = 0.023$; 95% CI, 1.161-7.312) (Table 2). The location of the lesions based on the portal venous blood supply according to Couinaud's segmental system was as follows: the medial and anterior segments, which was precisely expressed as the boundary between the medial and anterior segments based on CT images (n= 17) (Figures 1 and 2), anterior segment (n= 7), anterior and posterior segments (n= 3), lateral segment (n= 3), medial, anterior and posterior

segments (n= 2), medial segment (n= 1), posterior segment (n= 1), and lateral, medial, and anterior segments (n= 1). No lesion involved the caudate lobe (Table 3). The goodness-of-fit test showed the unequal distribution of the location of confluent fibrosis ($\chi^2_5 = 28.26$, $P < .0001$; the last three locations [n=1] were categorized as others).

The location based on the hepatic venous drainage was as follows: MHV drainage area (n= 21) (Figures 1 and 2), RHV drainage area (n= 8), LHV drainage area (n= 3), and MHV and RHV drainage areas (n= 3) (Table 4). The goodness-of-fit test showed the unequal distribution of the location of confluent fibrosis ($\chi^2_3 = 24.77$, $P < .0001$).

Discussion

In this study, we accessed confluent hepatic fibrosis in patients with cirrhosis in relation to the portal and hepatic venous anatomy. The results showed confluent fibrosis in 3.4% of patients with cirrhosis. The lesions were most commonly seen in the patients with advanced and/or alcoholic cirrhosis,

and in MHV drainage area in terms of hepatic venous drainage or at the boundary between medial and anterior segments in terms of portal venous supply. In general, the MHV receives blood mainly from the medial segment and ventral portion of the anterior segment [22], and the most common site of confluent fibrosis was confirmed to be within the MHV drainage area.

The prevalence of confluent fibrosis in our study (3.4%, 30 of 879 patients) is lower than that in Ohtomo's study [4], thought to be due to the difference in the stage of the cirrhosis. Two-thirds of the patients were classified as Child-Pugh class A in our study, and this study population consisted largely of less advanced cirrhosis as compared with the patients with relatively advanced cirrhosis who underwent liver transplantation in Ohtomo's study.

The developmental mechanism of confluent fibrosis has been speculated to be related to impaired portal microcirculation [4, 22]. It is based on the fact that decreased or absent portal blood supply was detected on CT during arterial portography [23], and that the reduction of portal flow resulted in loss of the volume of hepatocytes with increased fibrosis and segmental

atrophy of the liver [24]. However, confluent fibrosis was located most commonly at the boundary between the anterior and medial segments. The simultaneous reduction of portal blood supply in both the medial and ventral portions of the anterior segment may be difficult to explain based on a hypothetical disproportion of the portal blood supply. Other factors such as so-called streaming of the portal blood flow with the predominant splenic venous blood containing relatively large levels of insulin and other pancreatic hormones supplying the lateral segment [25], or the expected turbulent hepatopetal portal flow at the umbilical portion observed on ultrasound resulting in reduced portal flow to the medial segment [26] may also be implicated.

On the other hand, it is well known that when hepatic venous flow is obstructed, the portal flow in the obstructed segment is markedly reduced or even reversed resulting in the same hemodynamic conditions as in intrahepatic portal venous occlusion [11, 12]. Indeed, the intrahepatic venous flow obstruction also induces marked atrophy of the obstructed liver

parenchyma as commonly observed in Budd-Chiari syndrome [27].

The hepatic veins, unlike portal veins, are not surrounded by fibrous tissue that protects against external compression, and, therefore, stricture and/or obstruction due to compression by regenerative nodules and/or fibrosis is more severe than that noted in portal veins in cirrhosis. Therefore, we thought that the disturbances of hepatic venous drainage present in cirrhosis might markedly affect hepatic morphology and found selective atrophy of the MHV drainage area in hepatitis C-related cirrhosis [14]. The possible causes of the selective volume reduction seen in the MHV drainage area were considered to be as follows: the length of the MHV is slightly shorter than that of the RHV, and the proximal diameter is the smallest among the three major hepatic veins in normal livers. In contrast, the total volume of the MVH drainage area is the largest among LHV, MHV and RHV drainage areas. As a result, the postsinusoidal pressure elevation in the MHV drainage area due to compression by regenerative nodules is expected to be larger than in the other areas [14].

As revealed in this study, the most common site of confluent fibrosis exactly corresponded to the selective atrophic hepatic venous drainage area in cirrhosis. Therefore, confluent fibrosis may be explained as an extreme form of the selective atrophy of the MHV drainage area in cirrhosis, although this study included a variety of etiologies of cirrhosis. This is also strongly supported by the fact that the confluent fibrosis was more frequently found in advanced cirrhosis. In addition, the fact that all confluent fibrosis was located in the subcapsular area, radiating from the central portion of the liver to the hepatic periphery [4, 5] is also well explained by the larger resistance of hepatic venous drainage due to the relatively longer distance.

Although fibrosis is a common change in cirrhosis, its histological pattern varies depending on the etiology of cirrhosis [3]. For example, fibrous septa bridging portal triads and central veins are often seen in viral infection–related cirrhosis. On the other hand, perivenular and perisinusoidal fibrosis is commonly seen in alcoholic cirrhosis, and cholestasis-induced liver injury shows biliary interface hepatitis including

fibroplasia in the portal area [28]. Furthermore, so-call regenerative nodules in cirrhosis that are carved by progressive hepatic fibrous bands [2] are classified as macro-, micro-, and mixed-nodular cirrhosis, and also tends to depend on the etiologies of the cirrhosis [19]. However, as cirrhosis progresses, the characteristic histologic features of various etiologies may be lost, and the features of specific types of cirrhosis may be indistinguishable from cirrhosis due to other causes [2]. Thus, not only the differences of a variety of etiologies but also blood flow disorders may strongly influence confluent fibrosis. In addition, a histopathological study of the segmental atrophy of the liver suggested that the lesion was strongly associated with vascular injury [30].

The characteristic imaging findings of fibrosis depending on the etiology of cirrhosis are also seen; for example, AIH shows mostly extensive reticular and/or confluent fibrosis [31], PBC frequently shows lace-like pattern fibrosis [32], and alcoholic cirrhosis occasionally shows confluent fibrosis [4] also demonstrated in this study. The distinct amount of histological fibrosis

promoted by metabolic production of alcohol in alcoholic cirrhosis [33] may have some relation with the difference in the appearance of fibrosis. Therefore, the amount of fibrosis depending on specific etiologies may have a substantial influence on confluent fibrosis.

Our study had several limitations. First, the diagnosis of cirrhosis was established with pathology in only two-thirds of the patients. Second, the diagnosis of confluent fibrosis was established by the imaging findings except for in the four patients who underwent liver transplantation or partial hepatectomy. Third, in some patients with cirrhosis classified as Child-Pugh class C, there was some difficulty with the identification of hepatic vessels because of low contrast between the liver parenchyma and hepatic vessels. The window level and width were adequately adjusted to detect the fine vessels.

Conclusion

Confluent fibrosis associated with liver cirrhosis was most commonly

located in the MHV drainage area, and may have a relation to the hepatic venous drainage.

Acknowledgements

This work was supported in part by Japan Radiological Society for "Confluent hepatic fibrosis in liver cirrhosis: possible relation with middle hepatic venous drainage (KJ-23-10)".

References

1. Friedman SL. Hepatic fibrosis: overview. Toxicology 2008; 254:120–9.

2. Wallace K, Burt AD, Wright MC. Liver fibrosis. Biochem Genet 2008; 411:1–18.

3. Faria SC, Ganesan K, Mwangi I, Shiehmorteza M, Viamonte B, Mazhar S, et al. MR imaging of liver fibrosis: current state of the art. Radiographics 2009; 29:1615–35.

4. Ohtomo K, Baron RL, Dodd GD 3rd, Federle MP, Miller WJ, Campbell WL, et al. Confluent hepatic fibrosis in advanced cirrhosis: appearance at CT. Radiology 1993; 188:31–5.

5. Ohtomo K, Baron RL, Dodd GD 3rd, Federle MP, Ohtomo Y, Confer SR. Confluent hepatic fibrosis in advanced cirrhosis: evaluation with MR Imaging. Radiology 1993; 189:871–4.

6. Brancatelli G, Baron RL, Federle MP, Sparacia G, Pealer K. Focal confluent fibrosis in cirrhotic liver: natural history studied with serial CT. AJR Am J Roentgenol. 2009; 192:1341–7.

7. Brancatelli G, Federle MP, Ambrosini R, Lagalla R, Carriero A, Midiri M, et al. Cirrhosis: CT and MR imaging evaluation. Eur J Radiol. 2007; 61:57–69.

8. Yoshimitsu K, Irie H, Aibe H, Tajima T, Nishie A, Asayama Y, et al. Pitfalls in the imaging diagnosis of hepatocellular nodules in the cirrhotic and noncirrhotic liver. Intervirology 2004; 47:238–51.

9. Kelekis NL, Makri E, Vassiou A, Patsiaoura K, Spiridakis M, Dalekos GN. Confluent hepatic fibrosis as the presenting imaging sign in nonadvanced alcoholic cirrhosis. Clin Imaging 2004; 28:124–7.

10. Matsuo M, Kanematsu M, Kondo H, Asano T, Tomimatsu H, Manabe T, et al. Confluent hepatic fibrosis in cirrhosis: ferumoxides-enhanced MR imaging findings. Abdom Imaging 2001; 26:146–8.

11. Murata S, Itai Y, Asato M, Kobayashi H, Nakajima K, Eguchi N, et al. Effect of temporary occlusion of the hepatic vein on dual blood in the liver: evaluation with spiral CT. Radiology 1995; 197:351–6.

12. Hiraki T, Kanazawa S, Mimura H, Yasui K, Tanaka A, Dendo S, et al.

Altered hepatic hemodynamics caused by temporary occlusion of the right hepatic vein: evaluation with Doppler US in 14 patients. Radiology 2001; 220:357–64.

13. Okuda K, Itai Y. Cirrhosis. In: Okuda K, editors. Hepatobiliary disease: pathophysiology and imaging. Oxford: Blackwell Science; 2001. pp.119–51.

14. Ozaki K, Matsui O, Kobayashi S, Sanada J, Koda W, Minami T, et al. Selective atrophy of the middle hepatic venous drainage area in hepatitis C-related cirrhotic liver: morphometric study by using multidetector CT. Radiology 2010; 257:705–14.

15. Ito K, Mitchell DG, Gabata T. Enlargement of hilar periportal space: a sign of early cirrhosis at MR imaging. J Magn Reson Imaging 2000; 11:136–40.

16. Awaya H, Mitchell DG, Kamishima T, Holland G, Ito K, Matsumoto T. Cirrhosis: modified caudate-right lobe ratio. Radiology 2002; 224: 769–74.

17. Ahn IO, de Lange EE. Early hyperenhancement of confluent hepatic fibrosis on dynamic MR imaging. AJR Am J Roentgenol. 1998; 171:901–2.

18. Yoshikawa J, Matsui O, Kadoya M, Gabata T, Arai K, Takashima T. Delayed enhancement of fibrotic areas in hepatic masses: CT-pathologic correlation. J Comput Assist Tomogr. 1992; 16:206-11.

19. Couinaud C, editor. Surgical anatomy of the liver revisited. Paris, France: Couinaud, 1989.

20. Cho A, Okazumi S, Makino H, Miura F, Ohira G, Yoshinaga Y, et al. Relation between hepatic and portal veins in the right paramedian sector: proposal for anatomical reclassification of the liver. World J Surg 2004; 28:8–12.

21. Kanemura E, Togo S, Shizawa R, Tanaka K, Shimada H. Subdivision of liver anterior segment into two units according to hepatic venous drainage. Hepatogastroenterology 2000; 47:1056–9.

22. Harbin WP, Robert NJ, Ferrucci JT. Diagnosis of cirrhosis based on regional changes in intrahepatic morphology: a radiological and pathological analysis. Radiology 1980; 135: 273–83.

23. Itai Y, Murata S, Kurosaki Y. Straight border sign of the liver: Spectrum

of CT appearances and causes. Radiographics 1995; 15:1089–102.

24. Starzl TE, Francavilla A, Halgrimson CG, Francavilla FR, Porter KA, Brown TH, et al. The origin, hormonal nature, and action of hepatotrophic substances in portal venous blood. Surg Gynecol Obstet 1973; 137:179–99.

25. Lawrance JA, McDermott VG, Paulson EK, Keogan MT, Delong DM, Meyers WC, et al. Zebra pattern: a diagnostically challenging hepatic parenchymal enhancement pattern at CT arterial portography. Radiology 1997; 203:115–9.

26. Rosenthal SJ, Harrison LA, Baxter KG, Wetzel LH, Cox GG, Batnitzky S. Doppler US of helical flow in the portal vein. RadioGraphics 1995; 15:1103–11.

27. Mathieu D, Vasile N, Menu Y, Van Beers B, Lorphelin JM, Pringot J. Budd-Chiari syndrome: dynamic CT. Radiology 1987; 165:409–13.

28. Portmann B, Nakanuma Y. Diseases of the bile ducts. In: MacSween RNM, Burt AD, Portmann BC, Ishak KG, Scheuer PJ, Anthony PP, editors. Pathology of the liver. 4th ed. London: Churchill Livingstone; 2002. pp.435-

506.

29. Brown JJ, Naylor MJ, Yagan N. Imaging of hepatic cirrhosis. Radiology 1997; 202:1–16.

30. Singhi AD, Maklouf HR, Mehrotra AK, Goodman ZD, Drebber U, Dienes HP, et al. Segmental atrophy of the liver: a distinctive pseudotumor of the liver with variable histologic appearances. Am J Surg Pathol. 2011; 35:364–71.

31. Bilaj F, Hyslop WB, Rivero H, Firat Z, Vaidean G, Shrestha R, et al. MR imaging findings in autoimmune hepatitis: correlation with clinical staging. Radiology 2005; 236:896–902.

32. Blachar A, Federle MP, Brancatelli G. Primary biliary cirrhosis: clinical, pathologic, and helical CT findings in 53 patients. Radiology 2001; 220:329–36.

33. Maher JJ. Hepatic fibrosis caused by alcohol. Semin Liver Dis 1990; 10:66–74.

Figure legends

Figure 1. 52-year-old man with alcoholic cirrhosis who is classified as Child-Pugh class B.

a Pre-contrast CT image shows a wedge-shaped low attenuation area accompanied by capsule retraction and volume loss, which was defined as confluent fibrosis (arrowhead).

b Arterial phase CT image shows less marked enhancement of the lesion than that of adjacent hepatic parenchyma (arrowhead).

c Portal Phase CT image shows trapped branches of P8 and P4 within confluent fibrosis (arrowhead). The lesion was located at the boundary between anterior and medial segments.

d Equilibrium-phase CT image shows trapped branches of MHV within confluent fibrosis (arrowhead). The lesion was located in MHV drainage area.

Figure 2. 67-year-old man with alcoholic cirrhosis who is classified as

Child-Pugh class B.

a Pre-contrast CT image shows a wedge-shaped low attenuation area accompanied by capsule retraction and volume loss, which was defined as confluent fibrosis (arrowhead).

b Arterial phase CT image shows early enhancement of the lesion (arrowhead).

c Portal Phase CT image shows trapped branches of P8 and P4 within confluent fibrosis (arrowhead). The lesion was located at the boundary between anterior and medial segments.

d Equilibrium-phase CT image shows branches of MHV trapped within confluent fibrosis (arrowhead). The lesion was located in MHV drainage area.

Tables

Table 1 Causes of liver cirrhosis and more details in 879 patients.

Table 2 Results of univariable analyses and stepwise multiple logistic regression analysis.

Stepwise multivariate logistic regression analysis included the variables which were significant in the univariable analyses. The results showed that the significant predictive factors of confluent fibrosis were alcoholic cirrhosis, Child-Pugh class C, and Child-Pugh class B.

Table 3 Location of confluent hepatic fibrosis in terms of portal venous supply.

The goodness-of-fit test showed the unequal distribution of the location of confluent fibrosis ($\chi^2_5 = 28.26$, $P < .0001$; the last three locations [n=1] were categorized as others). The confluent fibrosis was most commonly seen at the boundary between the medial and anterior segments.

Table 4 Location of confluent hepatic fibrosis in terms of hepatic venous drainage.

The goodness-of-fit test showed the unequal distribution of the location of confluent fibrosis ($\chi^2_3 = 24.77$, $P < .0001$). The confluent fibrosis was most commonly seen in MHV drainage area.

Table 1 Causes of liver cirrhosis and more details in 879 patients.

				Child-Pugh classification		
Cause of cirrhosis	Number of patients	M/F	Age	Child-Pugh class A	Child-Pugh class B	Child-Pugh class C
Hepatitis C virus infection	528	303/225	67.8 ± 9.8	399	85	44
Hepatitis B virus infection	122	91/31	61.4 ± 9.2	87	27	8
Alcoholism	114	97/17	62.2 ± 10.5	74	27	13
Unknown etiology	36	15/21	68.6 ± 12.1	21	9	6
PBC	31	9/22	68.2 ± 9.1	19	3	9
NASH	24	12/12	64.0 ± 12.3	20	3	1
AIH	15	4/11	64.9 ± 13.2	8	5	2
Hepatitis C and B virus infection	3	2/1	61.7 ± 11.6	2	0	1
Budd-Chiari syndrome	3	3/0	60.7 ± 10.1	2	1	0
Hepatitis C virus infection and alcoholism	2	2/0	60.5 ± 12.5	1	1	0
Wilson's disease	1	1/0	7.0 ± 0.0	0	0	1

Table 2 Results of univariable analyses and stepwise multiple logistic regression analysis.

	Existence of confluent fibrosis		Univariable analysis	Multiple logistic regression analysis		
Variables	(+)	(-)	P value	P value	Odds radio	95% confidence interval
Number of cases (n=879)	30	849	-	-		
Male/Female	24/6	515/334	0.036	0.167	-	-
Age	62.6±10.3	66.1±10.6	0.039	0.520	-	-
Child-Pugh class A (n=633)	11	622	.0001	1	-	-
Child-Pugh class B (n=161)	9	152		.023	2.914	1.161-7.312
Child-Pugh class C (n=85)	10	75		.0001	6.946	2.765-17.446
Alcoholism/others	17/13	97/752	.0001	.0001	7.251	3.366-15.619

Stepwise multivariate logistic regression analysis included the variables that were significant in the univariable analyses. The significant predictive factors of confluent fibrosis were alcoholic cirrhosis, Child-Pugh class C, and Child-Pugh class B.

Table 3 Location of confluent hepatic fibrosis in terms of portal venous supply.

Location	Number of Lesions
Medial and anterior segments (boundary between the medial and anterior segments)	17
Anterior segment	7
Anterior and posterior segments	3
Lateral segment	3
Medial, anterior and posterior segments	2
Medial segment	1
Posterior segment	1
Lateral, medial, and anterior segments	1
Total (n=35)	35

The goodness-of-fit test showed the unequal distribution of the location of confluent fibrosis ($\chi^2_5 = 28.26$, $P < .0001$; the last three locations [n=1] were categorized as others). The confluent fibrosis was most commonly seen at the boundary between the medial and anterior segments.

Table 4 Location of confluent hepatic fibrosis in terms of hepatic venous drainage.

Location	Number of Lesions
MHV drainage area	21
RHV drainage area	8
LHV drainage area	3
MHV and RHV areas	3
Total	35

The goodness-of-fit test showed the unequal distribution of the location of confluent fibrosis ($\chi^2_3 = 24.77$, $P < .0001$). The confluent fibrosis was most commonly seen in MHV drainage area.

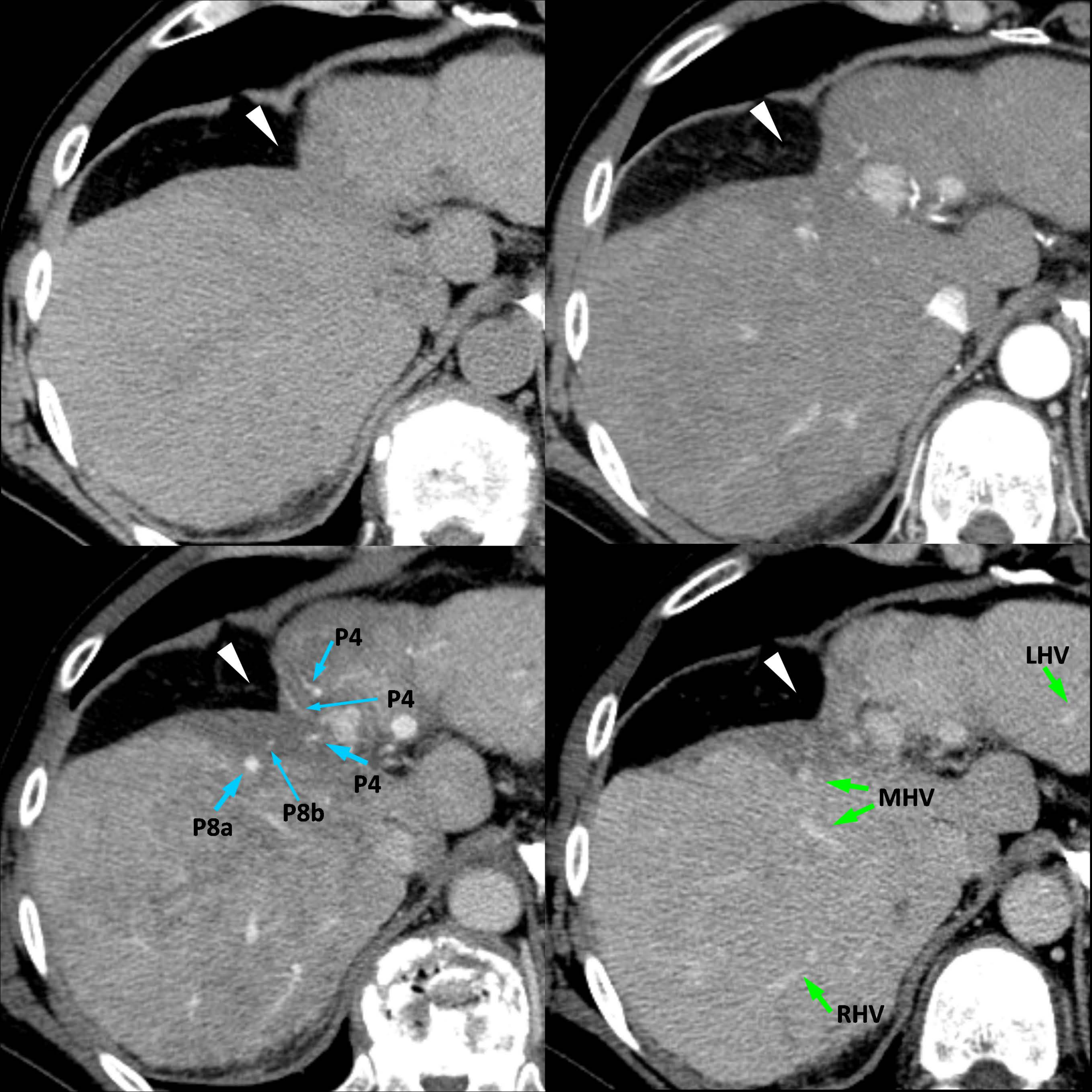
P4
P4
P4
P8a
P8b
LHV
MHV
RHV

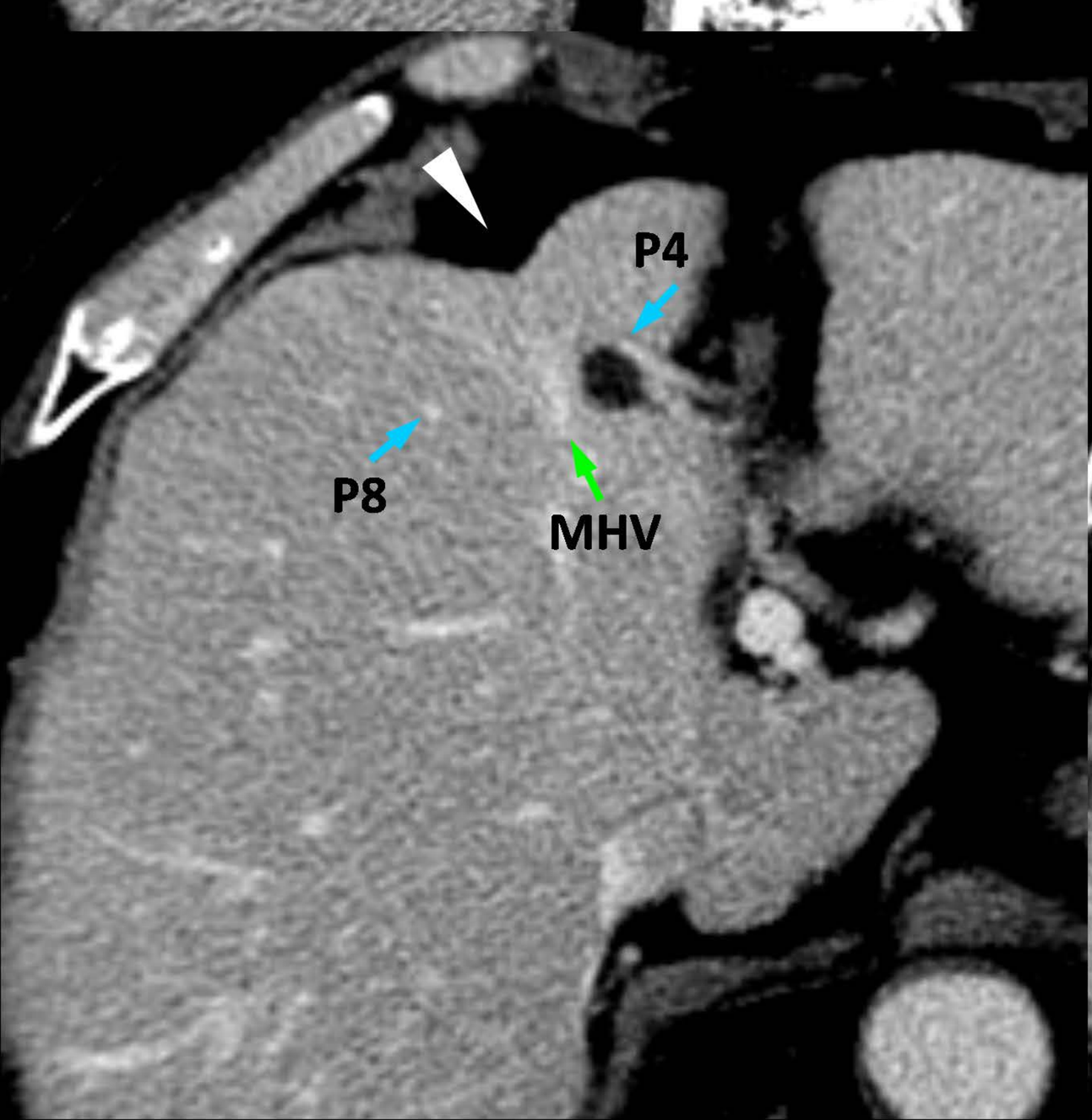
P4
P8
MHV

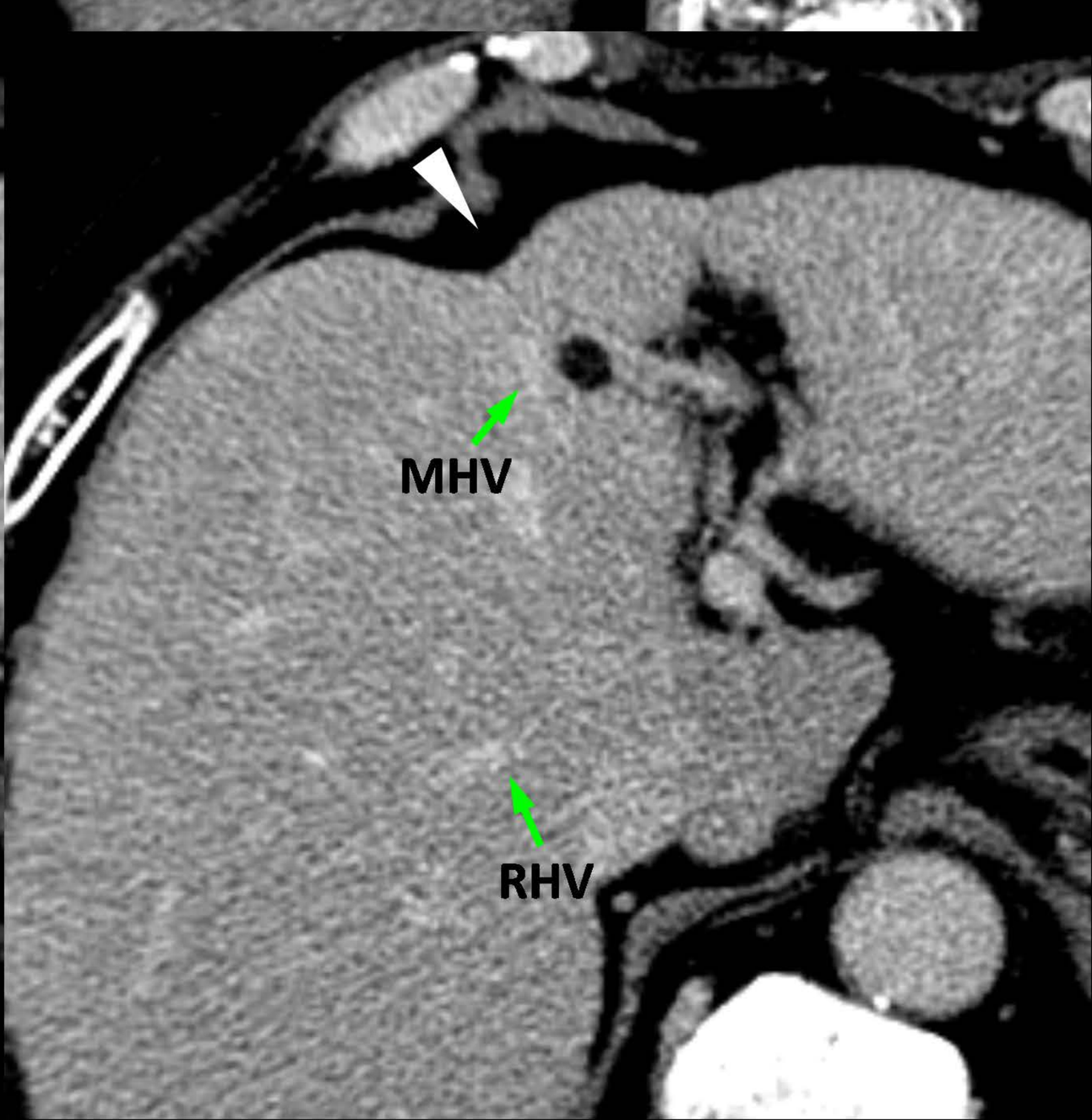
MHV
RHV